The 2010 IEEE/RSJ International Conference on
Intelligent Robots and Systems
October 18-22, 2010, Taipei, Taiwan

Closed-Loop Precise Turning Control for a BCF-Mode Robotic Fish

Zongshuai Su, Junzhi Yu, Min Tan, and Jianwei Zhang

Abstract— **This paper deals with a novel closed-loop maneuvering control method to enhance the turning precision and turning response speed of a robotic fish propelled via the body and/or caudal fin (BCF) mode. Although the BCF propulsion is favorable for the cases requiring greater thrust and accelerations, its maneuverability can be compensated by effective turning control. In our method, the turning maneuver is divided into three phases: the bending, holding, and unbending phases. After much consideration on turning details, the functions of each phase and the basic control laws are further identified. Results of experiments on in-situ direction tracking and direction maintaining verify the effectiveness of the proposed turning control.**

I. Introduction

Recent years have witnessed significant progress in the field of bio-inspired swimming robots, i.e., robotic fish [1], [2]. With regard to swimming-oriented swimming control, various control method are proposed, such as body wave and offsets based control method [3], [4], central pattern generators (CPGs) [5], etc. These methods are used in different kinds of fish models, which generally fall under two major categories of propulsion: body and/or caudal fin (BCF) mode [3], [5], [6] and median and/or paired fin (MPF) mode [7]. As is well recognized, the BCF mode is adept in cruise and acceleration; whereas it is poorer in precise maneuver than the MPF mode does [8]. With the purpose of acquiring enhanced maneuverability in the BCF-mode swimming, the turning maneuver enabling a closed-loop control becomes the subject of this paper.

The average behaviors of turning maneuver, up to the present, has been well studied, such as the turning angle rate, the turning radius, etc [3], [6]. These parameters are measured during a steady state while the robotic fish is swimming in a circle, controlled by open-loop control methods. In general, these open-loop methods utilize periodical control commands so that the robot falls into a dynamic steady state so long as the ambient environment is in a steady state. For instance, the water is still. However, these constant parameters are useless for achieving any desired direction via the turning maneuver. In fact, the actual turning maneuver is an unsteady state, namely, a transient state, which has no constant parameters and only continues for a short period of time. Therefore, it is only closed-loop control method that can perform precise turning control of BCF mode. For the purpose of precise control, the process of turning maneuver should be studied in details.

Popular opinion holds that fish turning of BCF mode can roughly be divided into three phases.

- **The bending phase**. The fish body transfers from a straight state to a curved state.
- **The holding phase**. The fish body maintains the curved state. When turning with a forward speed, the holding phase can be superposed by a fish body wave.
- **The unbending phase**. The fish body returns from the curved state back to the straight state.

As is discussed above, when it is focused on average behaviors, such as the average turning rate or turning radius [3], [6], the holding phase will be the key point of the research. To ensure a smooth transition of gaits [5], [9], the bending phase and the unbending phase should be paid more attention. In our research, it is found that the crucial problem of turning is the direction of the fish head, which in most cases is defined as the goal direction or the final direction, only when the fish body has stretched back to a straight form. Any phase of turning is able to change the direction of the head. However, it is evident that, the unbending phase is the last phase which can influence the final direction during a turning maneuver. Hence, the key point of turning precision can be concentrated on the unbending phase. On the other hand, the key point of response speed is the bending phase, which reflects the agility of the fish. Therefore, our research will focus on the bending and unbending phases.

It is extremely difficult to find out the relation between arbitrary movements of the fish body and the corresponding turning angles, owing to the complexity of the hydrodynamics. A theoretical framework of the turning motion is presented in [10]. However, the applied equations are so complicated that it is somewhat both difficult to understand and compute in real-time. Nevertheless, it is quite easy to find out the way that can minimize the turning angle which is induced in the unbending phase, and the way that can maximize the turning angle in the bending phase. Details will be discussed in Section II.

The rest of the paper is organized as follows. In Section II, the details of turning maneuver of BCF mode and the closed-loop control strategy are discussed. Section III provides the experimental results and discussions on in-situ turning maneuvers. Finally, Section IV concludes this work and suggests the future work.

This work was partly supported by the National Natural Science Foundation of China (60775053, 60865004), the National 863 Program (2007AA04Z202), and the Beijing Natural Science Foundation (4082031, 4102063).

Z. Su, J. Yu, and M. Tan are with the Laboratory of Complex Systems and Intelligence Science, Institute of Automation, Chinese Academy of Sciences, Beijing 100190, China. Currently J. Yu is also a guest researcher supported by the Alexander von Humboldt Foundation with the Department of Informatics, University of Hamburg, Germany. Corresponding email: zongshuai.su@ia.ac.cn

J. Zhang is with the the Department of Informatics, University of Hamburg, Germany zhang@informatik.uni-hamburg.de

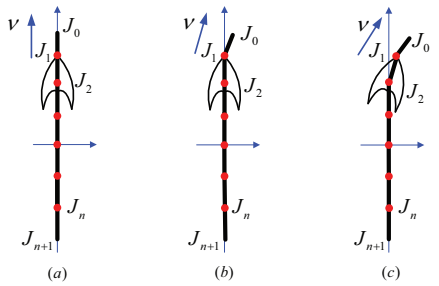

Fig. 1. The multilink model of the robotic fish and the illustration of a right turn while swimming forward. (a) The body wave is suspended to start a turning maneuver. (b) J_0 starts to bend in order to increase the angle rate α. (c) J_1 takes the role of active joint to bend to further increase the turning rate of the fish.

II. Closed-loop Turning Control

The whole turning movement of the BCF mode, as is mentioned before, consists of three phases. However, the same phase may be different due to the fish state:

- **Swimming forward**. This simply means a turning maneuver during the forward swimming. In this case, the turning radius r should be carefully considered. If the desired radius is relatively small, the fish can get to its goal direction only by the bending phase. If r is big enough, the fish will take advantage of the holding phase to achieve the goal direction, and restore to straight form by means of the unbending phase.
- **Staying in situ**. This does not mean the fish is still before turning maneuvers, but only implies a zero radius turning. In this case, the bending phase contributes almost all the turning angle, for the holding phase is quite short. The unbending phase is designed to add minimum disturbance to the final direction.

Specifically, each phase will be discussed in the following parts. It is worth noting that, similar to our previous work [3], the adopted robotic fish is modeled as a multilink system, as is illustrated in Fig. 1. It has n joints $J_1, J_2, ..., J_n$ and $n+1$ links $L_0, L_1, ..., L_n$. The rostral and caudal points are denoted as J_0 and J_{n+1} for convenience. To avoid confusion, the term "turning angle θ" and "turning rate α" will always mean the turning of the fish head, while "rotating angle θ_i" and "rotating rate α_i" will always indicate the rotation of the joint J_i $(i = 1, 2, ..., n)$.

A. The Bending Phase of Turning while Swimming Forward

With a forward speed $v > 0$, it is easier to utilize a rudder to change the direction of the fish, and the largest rudder is the anterior part of the fish body. Therefore, J_i will bend in sequence to achieve the desired turning radius r. Because of underlying complexity in turning hydrodynamics, the relationship between r and each joint's bending angle θ_i $(i = 1, 2, ..., n)$ is tough to find out. However, through realtime feedback and carefully designed control algorithms, it is easy to satisfy the value of r.

In kinematics, r can be calculated by $r = \frac{v}{\alpha}$, where v and α are the forward speed and turning rate of fish, respectively.

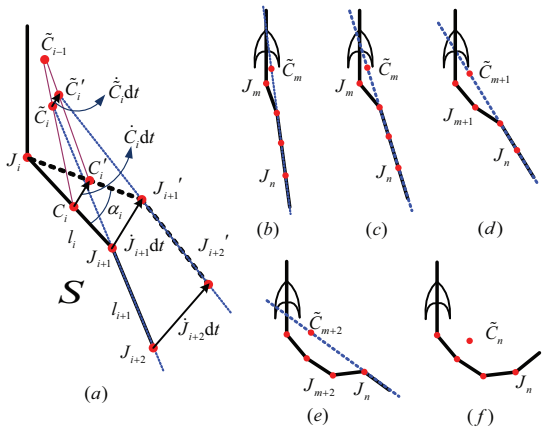

Fig. 2. (a) The recurrent calculation of α_{i+1} according to α_i. J_*' represents the new position of J_* after a time interval of dt. (b)∼(f) illustrate the bending phase of in-situ turning, where $J_m, J_{m+1}, ..., J_n$ take the role of active joint in sequence.

In order to concentrate on the turning rate, the body wave should be suspended. Since the bending phase is relatively short, the speed v will not decrease too much. At the very beginning, α is obviously zero. By bending $J_1, J_2, ..., J_m$ $(m \leqslant n)$ in sequence, α will progressively increase(see Fig. 1). When α arrives at the desired or its maximum value (if $m = n$), the bending phase will stop.

B. The Bending Phase of In-situ Turning

Without a forward speed, the propulsion of turning comes merely from the deformation of fish body. With a view to achieve the maximum turning angle, the lateral force should be maximized. Each link L_i can be modeled as a flat plate. Based on simplified hydrodynamics, when the speed is constant, the maximum force comes only if the front face area is maximized, i.e., only if each link has a lateral movement perpendicular to its longitudinal axis. Therefore, if the rear links make sure that their own longitudinal axis is parallel to the line between itself and the center of mass of the fish (referred to as the parallel condition), then the lateral forces can be maximized(see Fig. 2(b) ∼ Fig. 2(f)).

Let J_m denote the starting joint, whose rotating rate is α_m. J_m is called the active joint, and $J_{m+1}, ..., J_n$ the passive joints. There exists only one active joint at the same time. When J_m has bent to its limit, J_{m+1} will take the role of active joint. If the turning maneuver does not start from a straight body, the fish body behind the active joint should firstly recover to a straight line, in order to obtain a larger lateral area. In this case, these passive joints should rotate with a modest angle rate (e.g., as same as that of the active joint), in order to add as few disturbances as possible to the fish. After this adjustment, the passive joints can be calculated as follow.

The coordinate system is fixed in the fish head. As is illustrated in Fig. 2(a), let C_i, l_i $(i = 0, 1, ..., n)$ denote the center of mass and the length of each link L_i, respectively. Let $\widetilde{C}_i$ denote the resultant center of mass of links $L_0, ..., L_i$. It is obvious that $\widetilde{C}_0 = C_0$. Let $\dot{C}_i$, $\dot{\widetilde{C}}_i$, $\dot{J}_i$ denote the velocity vector of each point, and let $\mathscr{R}_{\alpha_i}$ denote the differentiation

of rotation transformation. It follows that

$$\dot{C}_i = \mathscr{R}_{\alpha_i}(\overrightarrow{J_iC_i}), \tag{1}$$

where $\overrightarrow{J_iC_i}$ stands for the vector from point J_i to C_i; and

$$\dot{J}_{i+1} = \mathscr{R}_{\alpha_i}(\overrightarrow{J_iJ_{i+1}}). \tag{2}$$

Details of derivation are illustrated in the Appendix.

The total mass $\widetilde{m}_{i-1}$ of $L_0,...,L_{i-1}$ and the mass m_i of L_i are obviously constant, so that the calculation of $\widetilde{C}_i$ is

$$\widetilde{C}_i = \lambda_i\overrightarrow{\widetilde{C}_{i-1}C_i} + \widetilde{C}_{i-1}, \tag{3}$$

where $\lambda_i = \frac{m_i}{\widetilde{m}_{i-1}+m_i}$ is a constant ratio. After a time interval of $\mathrm{d}t$, C_i goes to C_i', and $\widetilde{C}_i$ to $\widetilde{C}_i{}'$, but the ratio λ_i is constant, hence $\triangle\widetilde{C}_{i-1}\widetilde{C}_i\widetilde{C}_i{}' \sim \triangle\widetilde{C}_{i-1}C_iC_i'$, so that we can obtain

$$\dot{\widetilde{C}}_i = \lambda_i\dot{C}_i. \tag{4}$$

By the parallel condition, $\overrightarrow{J_{i+1}J_{n+1}}$ should go through $\widetilde{C}_i$, so that $\overrightarrow{J_{i+1}J_{n+1}}$ can go through the center of mass of the whole fish. Hence,

$$\begin{aligned} J_{i+2} &= \frac{l_{i+1}}{\left|\overrightarrow{\widetilde{C}_iJ_{i+1}}\right|}\cdot\overrightarrow{\widetilde{C}_iJ_{i+1}} + J_{i+1} \\ &= \frac{l_{i+1}}{\left|J_{i+1}-\widetilde{C}_i\right|}\cdot(J_{i+1}-\widetilde{C}_i) + J_{i+1}, \end{aligned} \tag{5}$$

and

$$\begin{aligned} J'_{i+2} &= \frac{l_{i+1}}{\left|\overrightarrow{\widetilde{C}_i{}'J'_{i+1}}\right|}\cdot\overrightarrow{\widetilde{C}_i{}'J'_{i+1}} + J'_{i+1} \\ &= \frac{l_{i+1}}{\left|J_{i+1}-\widetilde{C}_i+(\dot{J}_{i+1}-\dot{\widetilde{C}}_i)\mathrm{d}t\right|}\cdot\big[J_{i+1}-\widetilde{C}_i \\ &\quad +(\dot{J}_{i+1}-\dot{\widetilde{C}}_i)\mathrm{d}t\big] + J_{i+1} + \dot{J}_{i+1}\mathrm{d}t. \end{aligned} \tag{6}$$

$(\dot{J}_{i+1}-\dot{\widetilde{C}}_i)\mathrm{d}t$ is very small, so that

$$\frac{l_{i+1}}{\left|\overrightarrow{\widetilde{C}_iJ_{i+1}}\right|} \approx \frac{l_{i+1}}{\left|\overrightarrow{\widetilde{C}_i{}'J'_{i+1}}\right|}, \tag{7}$$

and we denote it as A_i. (6) $-$ (5), we have

$$\mathrm{d}J_{i+2} = J'_{i+2} - J_{i+2} = A_i(\dot{J}_{i+1}-\dot{\widetilde{C}}_i)\mathrm{d}t + \dot{J}_{i+1}\mathrm{d}t, \tag{8}$$

so that the recurrence formula is

$$\dot{J}_{i+2} = A_i(\dot{J}_{i+1}-\dot{\widetilde{C}}_i) + \dot{J}_{i+1}. \tag{9}$$

Therefore, we can obtain the angle rate of J_{i+1} by

$$|\alpha_{i+1}| = \frac{\left|\dot{J}_{i+2} - \mathscr{R}_{\alpha_i}(\overrightarrow{J_iJ_{i+2}})\right|}{l_{i+1}}. \tag{10}$$

The detailed derivation of (10) is also shown in the Appendix. The rotating direction of α_{i+1} can be determined by the practical situation of the fish. When J_i arrives at its limit, J_{i+1} will be the active joint.

For real fish, when they only need to turn a small angle, they often choose a more posterior joint to obtain a longer arm of force. Whereas, in common robot applications, J_1 will always be the first active joint in a turning maneuver to simplify the control law.

C. The Holding Phase of Turning while Swimming Forward

In this phase, the linear velocity can be compensated by superposing the body wave to the curved fish body. The linear velocity can be accelerated by increasing the amplitude and/or the frequency of the body wave. However, the change of the amplitude implies the change of the shape of the body wave, which may add extra unstable factors to the turning maneuver. Hence, the most convenient way is to change the frequency only. In addition, the decrease of the velocity is very small after a short bending phase. Therefore, it is very easy to maintain the linear velocity.

D. The Holding Phase of In-situ Turning

Without a forward speed, the turning movement will soon stop if the fish body has stopped bending, so that this phase almost does not exist in the case of in-situ turning.

E. The Unbending Phase of Turning while Swimming Forward

This phase is the most important part in turning maneuvers, which directly concerns the final direction of the fish head. The main principle in this phase is to minimize the lateral force, so that the fish head can keep its direction.

The minimum front face area of each link during a yaw motion is its cross-section. Furthermore, the cross-section itself does not directly contact to the water, so that the hydrodynamic forces consist only of the friction drag and some other small factors. This advantage helps each link find its own pattern of motion: it should move directly after its previous joint, so that the drags encountered by each link can be as small as possible. Regarding it as a whole, the fish is restrained in a virtual "pipeline", as illustrated in Fig. 3(c) $\sim$ Fig. 3(e).

The coordinate system is set in the water. The velocity vector $\dot{J}_0$ and turning rate α_0 of the rostral point are the feedback of sensors. Hence by iterative algorithm, we can obtain $\dot{J}_i$ and α_i $(i = 1,2,...,n)$.

As is shown in Fig. 3, let S denote the trajectory of the fish body, namely, the polygonal curve from J_0 to J_{n+1}. Let $\dot{S}$ denote the unit tangent vector of S, namely, $|\dot{S}| = 1$. $\dot{S}$ represents the velocity direction of each point on S. However, S is not differentiable at J_i, so that we define

$$\dot{S}_i = \begin{cases} \dfrac{\overrightarrow{J_{i+1}J_i}}{|\overrightarrow{J_{i+1}J_i}|} = -\dfrac{\overrightarrow{J_iJ_{i+1}}}{l_i}, & \text{if } |\overrightarrow{J_{i+1}J'_i}| \geqslant l_i \\ \dfrac{\overrightarrow{J_{i+1}J_{i+2}}}{|\overrightarrow{J_{i+1}J_{i+2}}|} = \dfrac{\overrightarrow{J_{i+1}J_{i+2}}}{l_{i+1}}, & \text{if } |\overrightarrow{J_{i+1}J'_i}| < l_i \end{cases} \tag{11}$$

where J'_i represents the new position of J_i after a time interval of $\mathrm{d}t$. If $|\overrightarrow{J_{i+1}J'_i}| \geqslant l_i$, J'_{i+1} will be on $\overrightarrow{J_iJ_{i+1}}$, which means $\dot{S}_i$ is parallel to $\overrightarrow{J_iJ_{i+1}}$, as shown in Fig. 3(a). Similarly, J'_{i+1} will be on $\overrightarrow{J_{i+1}J_{i+2}}$, if $|\overrightarrow{J_{i+1}J'_i}| < l_i$ (see Fig. 3(b)).

In both Fig. 3(a) and Fig. 3(b), we have

$$\overrightarrow{J_{i+1}J'_i} = \dot{J}_i\mathrm{d}t - \overrightarrow{J_iJ_{i+1}}. \tag{12}$$

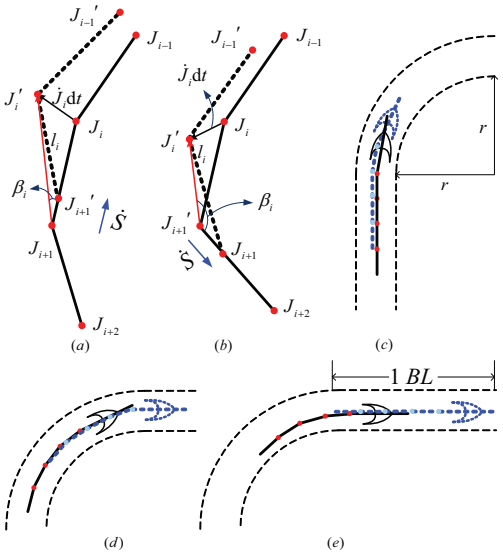

Fig. 3. During the unbending phase, every joint should keep in the trajectory of its directly anterior joint. Dashed lines represent the new positions after a time interval of dt, where dt is exaggerated for a better illustration. (a) and (b) illustrate the calculation of α_i, where α_{i-1} has been computed or sensed. (a) shows the case of $v > 0$, and (b) $v < 0$. If $v = 0$, α_i is set to zero. (c)∼(e) illustrate a right turning maneuver with the turning radius r.

In $\triangle J_i' J_{i+1} J_{i+1}'$, using cosine theorem, we have

$$|\overrightarrow{J_{i+1}J_i'}|^2 + |\dot{J}_{i+1}dt|^2 - 2\cos\beta_i |\overrightarrow{J_{i+1}J_i'}||\dot{J}_{i+1}dt| = l_i^2, \quad (13)$$

where

$$\cos\beta_i = \frac{\overrightarrow{J_{i+1}J_i'} \cdot \dot{S}_i}{|\overrightarrow{J_{i+1}J_i'}| \cdot |\dot{S}_i|}. \quad (14)$$

substituting (11), (12) and (14) into (13), and neglecting the second order small terms, we have

$$\dot{J}_i dt \cdot \overrightarrow{J_i J_{i+1}} + (\dot{J}_i dt - \overrightarrow{J_i J_{i+1}}) \cdot \dot{S} |\dot{J}_{i+1} dt| = 0. \quad (15)$$

Further neglecting the second order small term $\dot{J}_i dt |\dot{J}_{i+1} dt|$ and throwing off dt, we get

$$|\dot{J}_{i+1}| = \frac{\dot{J}_i \cdot \overrightarrow{J_i J_{i+1}}}{\overrightarrow{J_i J_{i+1}} \cdot \dot{S}}, \quad (16)$$

hence,

$$\dot{J}_{i+1} = |\dot{J}_{i+1}| \dot{S}. \quad (17)$$

Finally, we can obtain

$$|\alpha_i| = \frac{|\dot{J}_{i+1} - \dot{J}_{i-1} - \mathscr{R}_{\alpha_{i-1}}(\overrightarrow{J_{i-1}J_{i+1}})|}{l_i}. \quad (18)$$

The detailed derivation is similar to (10), also can be found in the Appendix.

If all the links follow their previous link exactly, then all the joints will return to straight angle, as soon as the fish head has passed a distance of 1 BL (body length)(see Fig. 3(e)). Therefore, if the forward speed is x BL/s, then the duration of the unbending phase is $\frac{1}{x}$ s.

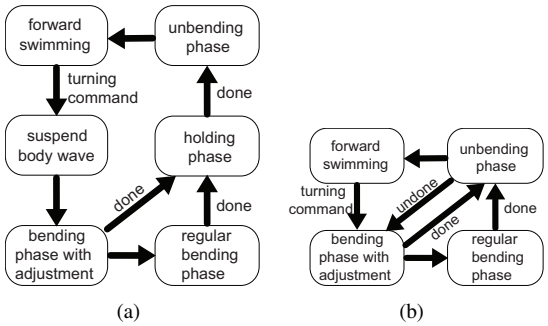

Fig. 4. The phase-transfer in turning while swimming(a) and in-situ turning(b). "done" indicates that the desired turning angle has been achieved, while "undone" means "has not been achieved". "adjustment" means to adjust the rear body to recover to a straight line.

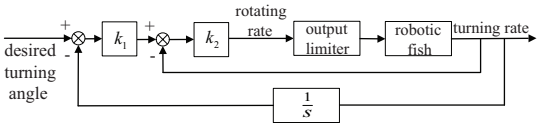

Fig. 5. The control block diagram of the rotating rate of the active joint. k_1 and k_2 are the proportional gains, and the output limiter is used to constrain the rotating rate.

F. The Unbending Phase of In-situ Turning

Without forward speed, $\dot{J}_0$ will be zero if no joint moves. Hence, the most anterior one of those curved joints should act as the active joint, similar to the bending phase. All the passive joint then can be calculated in the same way discussed above.

G. Closed-loop Control strategies

There are two levels of control system. The upper level is the transfer between phases, and the lower level is the detailed control of the turning angle. Fig. 4(a) shows the phase-transfer of turning maneuver while swimming, and Fig. 4(b) shows the in-situ turning.

In the lower level, simple PID algorithms are adopted to control the rotating rate of the active joint in both the bending and unbending phase. Fig. 5 illustrates the block diagram, where k_1 and k_2 are the proportional gains. At the beginning of the bending phase, a large angle deviation can yield fast rotating rate. Whereas, when nearing the end of the bending phase, the large turning rate will inhibit the rotating angle in order to slow down. At the beginning of the unbending phase, the large turning rate will instead result in a fast rotating rate, so that the turning rate can decrease rapidly. An output limiter is employed to constrain the final control signals not to exceed an upper bound. This upper bound is determined by the limitation of the servomotors, which cannot precisely track fast-varying signals.

III. Experiments and Discussions

The experiments are only about in-situ turning with a three-joint robotic fish equipped with a gyro [3]. At present, the used gyro is a single-axis yaw one fixed in the head of the robotic fish, which can only feed back the turning rate.

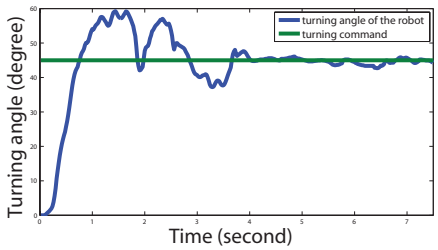

Fig. 6. The response diagram of the robotic fish after a command of 45° right turn. The data is collected from the gyro.

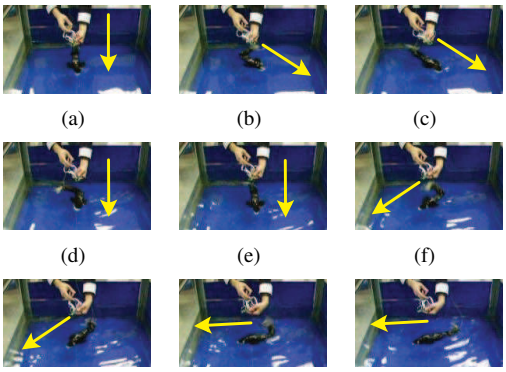

Fig. 7. Video snapshot sequence of direction tracking. The yellow arrow indicates the direction of the remote controller in the left hand. (a)∼(c) show the turning maneuver from the stationary state of the robotic fish, while (d)∼(i) show three loops of turning maneuvers. Some of them start when the unbending phase is still going on.

Without a sensor to feed the speed back, the robotic fish is unable to maintain its location during the turning maneuvers. Since the interest is mainly concentrated on the direction control, we tied a soft yellow rope to the peduncle of the robotic fish to limit its uncontrollable drift. The robotic fish is 35 cm long, weighing 0.84 kg, and using an Atmega128 as its main controller. During the lower level control, we choose a gain of $k_1 = k_2 = 50$ and limit the rotating rate by $225°/s$.

The control cycle is set to 20 ms, according to the requirement of the servomotor (S3003 from Futaba) which uses a 20 ms pulse width modulation (PWM). During each control cycle, the joint angles are calculated in the way discussed in Section II. The maximum bending angles are limited by the stiffness of the fish covering which is made out of lactoprene. They are 53°, 48° and 31°, respectively. The maximum turning rate is 300 °/s, restricted by the measurement range of the gyro (0 ∼ 300 °/s). The step response of a 45° right turn is shown in Fig. 6.

A. Direction Tracking

This task indicates the robotic fish should tightly follow the desired direction. The desired direction is sent to the robot from a remote controller, which is also equipped with the same gyro. Therefore, the mission for the robot is to make sure its own direction is parallel to that of the remote controller. Note that the remote controller sends its own direction to the robot once every 60 ms. During each control cycle, the robot compares its actual direction with the desired direction, and then apply the proposed control algorithm to eliminate the deviation.

In this experiment (see Fig. 7 or the movie), the robotic fish follows the remote controller very well, except the desired angle is too far to arrive in one loop of the turning maneuver. It strongly manifests the effectiveness of the proposed turning theories.

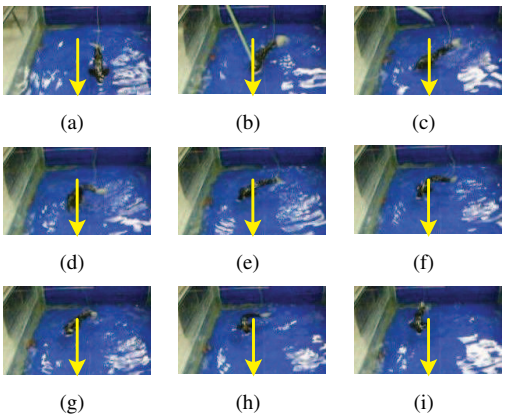

Fig. 8. Video snapshot sequence of direction maintaining. (a)∼(c) show that an external disturbance is exerted on the robotic fish, while (d)∼(i) show that the robotic fish returns to the desired direction.

B. Direction Maintaining

This task means that no matter what disturbances it encounters, it can return to its original direction as soon as possible without any control signals from outside the robot. This function is quite useful in practical applications, for instance, keeping formation of multi-robot system.

The original direction can be seen as the goal direction. When a disturbance occurs, it is quite easy for the robot to return to its original direction using the proposed turning strategy. In the experiment, the robotic fish is required to be parallel to the yellow arrow shown in Fig. 8 (or the middle line of the water tank in the movie). Disturbances are introduced to the robot in the forms of randomly changing its direction. As soon as it deviates the desired direction, it employs a turning maneuver to modify the bias, no matter the disturbance is still going on or not.

C. Discussions

The whole turning procedure can be simply depicted in this fashion: the fish can turn its head to its preferred direction as soon as possible. Once it achieves, it can begin the unbending phase to return its body to straight form, during which almost no disturbance will be appended. In many cases, the fish can reach its goal direction, only by one loop from bending to unbending. It should be remarked that the bending phase and even the holding phase can be arbitrary, as long as it can clear up the bias between the desired direction and its actual direction. No doubt, the most important factor is the unbending phase, which can

"lock" the direction of the fish, only allowing the forward movement.

Without a sensor to feed the forward speed back in real time, experiments of turning while swimming forward or removing the yellow rope to carry out real experiment of in-situ turning are currently unavailable. In addition, there are no pectoral fins on the robotic fish so that the forward speed cannot be fully decoupled from the turning angle rate.

On the other hand, the control of the joint angle is still open-loop, i.e., the PWM control of the servomotors has no feedback. When high rotating rate is required, the real joint angles of the servo motors cannot be regarded the same as the output any more. Therefore a feedback of joint angles should also be incorporated into the control laws so that the control quality can be further enhanced. Also, high rotating rate can introduce other problems, such as unignorable coriolis forces, more complex nonlinearity, etc. These should be well considered in order to achieve better performances. However, under the limitation of most servomotors, the robotic fish can hardly obtain a turning rate faster than $200^\circ/s$, which yields only a little unwanted complexity.

IV. Conclusions and Future Work

In this paper we first divide the process of turning maneuver into three phases based on the fundamental functions of each phase, and then propose the closed-loop control method. This method provides a fast and precise control of the fish direction. With emphasis on the unbending phase, the key point of precise turning control is uncovered. Finally, experiments of in-situ turning are carried out, which offer a vivid verification to the proposed theories.

In the near future, we will replace the gyro by a wide-range one, and build new fish covering to broaden the range of the rotation of each joint, and import new sensors to perceive the linear speed. New control algorithms including the feedback of joint angles will also be investigated. As a plus, pectoral fins will be fixed on the robotic fish, so that we can fulfill the precise control, not only for turning maneuvers, but also for the site-specific tasks.

References

[1] P. R. Bandyopadhyay, "Trends in biorobotic autonomous undersea vehicles," *IEEE J. Ocean. Eng.*, vol. 30, no. 1, pp. 109-139, 2005.

[2] K. A. Morgansen, B. I. Triplett, and D. J. Klein, "Geometric methods for modeling and control of free-swimming fin-actuated underwater vehicles," *IEEE Trans. Robot.*, vol. 23, no. 6, pp. 1184–1199, 2007.

[3] J. Yu, L. Liu, L. Wang, M. Tan, and D. Xu, "Turning control of a multilink biomimetic robotic fish," *IEEE Trans. Robot.*, vol. 24, no. 1, pp. 201–206, Feb. 2008.

[4] J. Yu, M. Tan, S. Wang, and E. Chen, "Development of a biomimetic robotic fish and its control algorithm," *IEEE Trans. Syst. Man Cybern. B, Cybern.*, 34(4): 1798–1810, 2004.

[5] A. J. Ijspeert, A. Crespi, D. Ryczko, J.-M. Cabelguen, "From swimming to walking with a salamander robot driven by a spinal cord model," *Sci.*, vol. 315, pp. 1416–1419, 2007.

[6] K. A. McIsaac and J. P. Ostrowski, "Open-loop verification of motion planning for an underwater eel-like robot," *Experimental Robotics VII*, LNCIS 271, 2001, pp. 271–280.

[7] C. Zhou and K. H. Low, "Locomotion planning of biomimetic robotic fish with multi-joint actuation," in *Proc. IEEE Int. Conf. Intell. Robot. Syst.*, St. Louis, MO, USA, Oct. 2009, pp. 2132–2137.

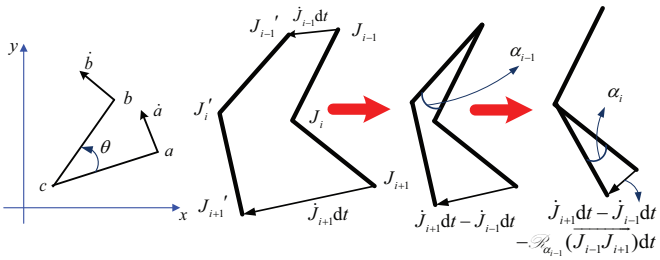

Fig. 9. (a) Illustration of the rotation transformation $\mathscr{S}_\theta$ from point a to b. $\dot{a}$ and $\dot{b}$ are the velocity vectors of a and b respectively. (b) The computation of the angle rate α_i, where J_{i-1}, J_{i+1} and α_{i-1} is given.

[8] R. W. Blake, "Fish functional design and swimming performance," *J. Fish Biol.*, vol. 65, pp. 1193–1222, 2004.

[9] J. Yu, M. Wang, M. Tan, and Y. F. Li, "Step function based turning maneuvers in biomimetic robotic fish," in *Proc. IEEE Int. Conf. Robot. Autom.*, Kobe, Japan, May 2009, pp. 3431–3436.

[10] Q. Hu, D. R. Hedgepeth, L. Xu, and X. Tan, "A framework for modeling steady turning of robotic fish," in *Proc. IEEE Int. Conf. Robot. Autom.*, Kobe, Japan, May 2009, pp. 2669–2674.

[11] Z. Su, J. Yu, M. Tan, and J. Zhang, "Bio-inspired design of body wave and morphology in fish swimming based on linear density," in *IEEE Int. Conf. Robot. Biomim.*, Guangxi, China, Dec. 2009, pp. 1803–1808.

Appendix

A. The Rotation Transformation and Its Differentiation

As is shown in Fig. 9(a), point a rotates around point c by an angle θ, arriving at point b. It can be calculated by

$$b = \mathscr{S}_\theta(\overrightarrow{ca}) + c = \mathscr{S}_\theta(a-c) + c, \tag{19}$$

where $\mathscr{S}$ is the rotation transformation. Written in matrix form, it becomes

$$\begin{bmatrix} x_b \\ y_b \end{bmatrix} = \begin{bmatrix} \cos\theta & -\sin\theta \\ \sin\theta & \cos\theta \end{bmatrix} \begin{bmatrix} x_a - x_c \\ y_a - y_c \end{bmatrix} + \begin{bmatrix} x_c \\ y_c \end{bmatrix}. \tag{20}$$

If the angle rate is α, i.e., $\dot{\theta} = \alpha$, then we have

$$\dot{b} = (\mathscr{S}_\theta(a-c) + c)' = \mathscr{S}'_\theta(a-c), \tag{21}$$

where

$$\begin{aligned} \mathscr{S}'_\theta &= \begin{bmatrix} \cos\theta & -\sin\theta \\ \sin\theta & \cos\theta \end{bmatrix}' = \begin{bmatrix} -\sin\theta & -\cos\theta \\ \cos\theta & -\sin\theta \end{bmatrix} \cdot \dot{\theta} \\ &= \begin{bmatrix} -\sin\theta & -\cos\theta \\ \cos\theta & -\sin\theta \end{bmatrix} \cdot \alpha. \end{aligned} \tag{22}$$

If $\theta = 0$, we obtain

$$\dot{a} = \dot{b}\big|_{\theta=0} = \begin{bmatrix} 0 & -1 \\ 1 & 0 \end{bmatrix} \cdot \alpha \cdot (a-c) = \mathscr{R}_\alpha(\overrightarrow{ca}), \tag{23}$$

where $\mathscr{R}_\alpha = \begin{bmatrix} 0 & -1 \\ 1 & 0 \end{bmatrix} \cdot \alpha$ is the differentiation of the rotation transformation $\mathscr{S}$. Therefore, $\mathscr{R}_\alpha(\overrightarrow{ca})$ represents the velocity vector of point a. Similarly, (1) and (2) can be derived.

B. The Calculation of Angle Rate

From (23), we can obtain

$$|\alpha| = \frac{|\dot{a}|}{\left|\begin{bmatrix} 0 & -1 \\ 1 & 0 \end{bmatrix} \cdot \overrightarrow{ca}\right|} = \frac{|\dot{a}|}{|\overrightarrow{ca}|}. \tag{24}$$

As is shown in Fig. 9(b),the real differentiation of J_{i+1} can only be calculated by subtracting the component of $\dot{J}_{i-1}$ and $\mathscr{R}_{\alpha_{i-1}}(\overrightarrow{J_{i-1}J_{i+1}})$. Therefore, (18) is derived. Since the coordinate system is fixed on the fish head in the bending phase, so that the translation movement of J_i in Fig. 2(a) is zero. Thus, (10) is derived.